Título del artículo:

Estimation of different ripening stages of Fuji apples using image processing and spectroscopy based on the majority voting method

Autores:

Razieh Pourdarbani*, Sajad Sabzi, Davood Kalantari, Jitendra Paliwal, Brahim Benmouna, Ginés García-Mateos*, José Miguel Molina-Martínez

Revista:
Computers and Electronics in Agriculture

Referencia:
Computers and Electronics in Agriculture, Vol. 176, 2020, 105643

DOI de la versión publicada:
https://doi.org/10.1016/j.compag.2020.105643

Estimation of different ripening stages of Fuji apples using image processing and spectroscopy based on the majority voting method

Razieh Pourdarbani [1], Sajad Sabzi [1], Davood Kalantari [2], Jitendra Paliwal [3], Brahim Benmouna [4], Ginés García-Mateos [4*] and José Miguel Molina-Martínez [5]

[1] Department of Biosystems Engineering, College of Agriculture, University of Mohaghegh Ardabili, Ardabil 56199-11367, Iran; r_pourdarbani@uma.ac.ir (R.P.), s.sabzi@uma.ac.ir (S.S.)

[2] Department of Mechanics of Biosystems Engineering, Faculty of Agricultural Engineering, Sari Agricultural Sciences and Natural Resources University, Mashhadsar, Iran; d.kalantari@sanru.ac.ir

[3] Department of Biosystems Engineering, E2-376 EITC, University of Manitoba, Winnipeg, MB, Canada; J.Paliwal@Umanitoba.ca

[4] Computer Science and Systems Department, University of Murcia, 30100 Murcia, Spain, brahim.benmouna@um.es (B.B.), ginesgm@um.es (G.G.-M.)

[5] Food Engineering and Agricultural Equipment Department, Technical University of Cartagena, 30203 Cartagena, Spain; josem.molina@upct.es

[*] Corresponding author: ginesgm@um.es; Tel.: +34 868 888 530 (G.G.-M.)

Abstract

Non-destructive determination of the different stages of fruit ripening has important advantages over traditional methods, such as selective robotic harvesting or adapting fertilization operations depending on the ripening stage. In this regard, the purpose of the present study was to investigate the non-destructive estimation of the ripening stages of Fuji apples combining different classifiers with the majority voting (MV) method. This process is based on five constituent classifiers, including hybrids of artificial neural network (ANN) classifiers adjusted with the genetic algorithm, the particle swarm optimization algorithm and the firefly algorithm, and classifiers based on support vector machines, and the k-nearest neighbor algorithm. The input of the MV classifiers consists of four alternatives: (1) color data extracted from the second channel of L*a*b* color space, and the hue angle in L*a*b*; and multispectral data including wavelengths ranging: (2) from 465 to 485 nm; (3) from 675 to 700 nm; and (4) from 870 to 890 nm. The first two ranges are in the visible spectrum, while the second is within the near-infrared. To evaluate the reliability of the MV method, the classification procedure was repeated 1000 times with different seeds. In order to assess the obtained performance, the proposed method has been compared with an alternative technique based on an ANN classifier, in this case using all the spectral data in the range from 450 to 1000 nm, and with the hyperparameters adjusted by a grid search. The results indicate that the correct classification rate of the MV method using color data, and using spectral data from 465 to 485 nm, 675 to 700 nm, and 870 to 890 nm were 95.12%, 99.37%, 97.56% and 97.80% respectively, while the correct classification rate of the ANN method including all the spectral data from 450 to 1000 nm reached an average classification of 92.12%. Thus, the optimal

selection is the MV method using spectral information from 465 to 485 nm, which is able to achieve a very accurate result, feasible to be used in practical applications.

Keywords: Color spaces; spectral data; non-destructive estimation; majority voting method; hybrid artificial neural network.

1. Introduction

Ripening is the main indicator of the shelf life and quality of fruits and vegetables (Lamikanra, 2002; Sabzi et al., 2013). Unripe fruits and vegetables have limited shelf life in the face of mechanical damage, softening, and physiological and microbiological disorders, which in turn can cause significant economic losses. Therefore, the importance of quality control, especially with non-destructive methods in agri-industry and in the global economy, is increasing (Pourdarbani et al., 2019; Pourdarbani et al., 2020). However, ripeness estimation becomes an important challenge when the appearance of the fruit is not related to its ripeness. Of course, human experts are capable of recognizing the ripening state, but it can be very expensive and time consuming.

Different methods (both destructive and non-destructive) have been proposed to determine fruit ripening in the literature. Destructive methods include measurement of properties such as mechanical and chemical features of the fruits (e.g. soluble solids), while non-destructive methods include other types of sensors such as optical, multispectral and hyperspectral methods. Hyperspectral imaging systems are expensive and require a sophisticated proprietary hardware system to run. Besides, the use of this high dimensional information can potentially require hundreds of megabytes for small size datasets. All these factors greatly increase the cost of receiving and processing the spectral data. So, the simplest and most practical approach is to use small-scale spectral data or effective spectral data. For this reason, the focus of this paper is to find these small spectral intervals that are the most effective for the ripening classification.

Visible and near-infrared spectroscopy (VIS-NIR) has been used for the estimation and prediction of the chemical properties of fruits and vegetables by various researchers (Liu et al., 2015; Bizzani et al., 2017; Ncama et al., 2017; Torres et al., 2017; Arendse et al., 2018; M. Cavaco et al., 2018). For example, Sabzi et al. (2019) developed an algorithm for identifying apples (of Red Delicious variety) in aerial images, and estimating their ripening state among four possible classes: unripe, half-ripe, ripe, and over-ripe. The proposed method was based on color properties and ANN optimized with metaheuristic genetic algorithms. The results showed an accurate classification rate of 97.88%, and values of the receiver operating characteristic (ROC) curve above 0.99 for all classes. Fernández-Novales et al. (2019) used a VIS-NIR spectrometer to estimate the amino acid content of grapes during ripening. Partial least squares (PLS) were used to create calibration, validation and prediction models. The best performance, with a coefficient of determination, R^2, around 0.60, was observed for lysine, asparagine, tyrosine and proline in the ranges of 570-1000 nm and 1100-200 nm. Adi et al. (2019) determined the relationships between the physical and chemical properties of the plantain and its ripening stages as a quality predictor. Three fruits were sampled every two days and observed for color, texture, pulp, moisture, pH, acidity, and Brix. There was a positive correlation between ripening stage and weight, pulp and color changes, and a negative correlation with respect to pH and dry matter. Adebayo et al. (2016) proposed a method for non-destructive estimation of qualitative properties and classification of banana based on ripening stage using optical properties. Five wavelengths of 532, 660, 785, 830, and 1060 nm were used to predict fruit quality. The results showed that there was a high correlation between the optical properties and the ripening stages of the bananas at 532, 660 and 785 nm wavelengths, with an accuracy of 97.53%. Cardenas-Perez et al. (2017) evaluated and estimated physicochemical properties of 114 golden delicious apple samples using a computer vision system. In order to extract the color properties, different color spaces were studied and finally, it was determined that the most suitable color space was CIE L*a*b*. The results showed that using a combination of color and chemical properties, it would be possible to accurately estimate the ripening stages of apples.

The purpose of the present study is to propose a novel non-destructive algorithm based on a reduced set of spectral data and a combination of classifiers using the majority voting rule, for the estimation of different ripening stages of Fuji apples, including unripe, half-ripe, ripe and over-ripe. As mentioned, non-destructive methods have received much interest due to their ability to monitor fruits during the cropping cycle. The ensemble classifier consists of five constituent classifiers: three hybrid methods of artificial neural networks (ANN) and the genetic algorithm, particle swarm optimization algorithm, and the firefly algorithm; and two classifiers using support vector machines (SVM) and the k-nearest neighbor algorithm. To assess the effectivity of selecting a reduced range of the spectrum, the obtained results are compared with an ANN classifier using all the available spectral data from 450 to 1000 nm, whose hyperparameters are manually optimized by trial and error.

2. Materials and Methods

The research process carried out in the present work to design a new method for the estimation the ripening stages of Fuji apples is outlined in Fig. 1. This process consists of 6 main steps: (i) collecting the apple samples according to the indication of the experts; (ii) extracting the spectral information for each sample; (iii) preprocessing the obtained data; (iv) extracting color information based on the CIE L*a*b* color space; (v) creating the basic classifiers based on color and on small bands of the spectrum; and (vi) combining the classifiers with the majority voting (MV) method.

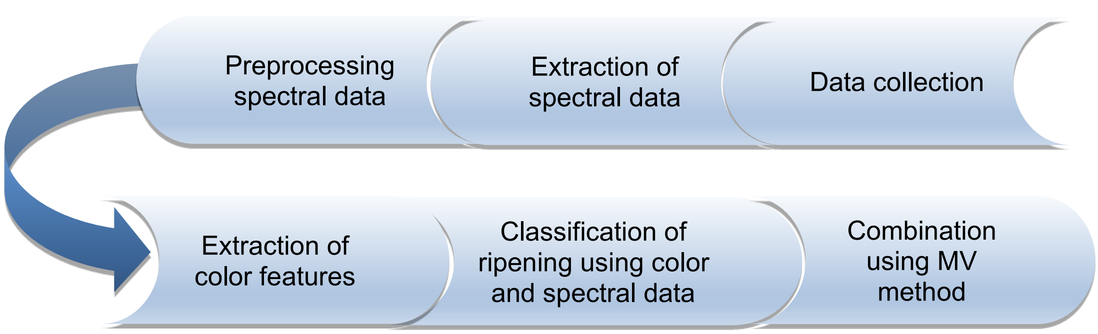

Fig. 1. Global outline of the research process applied in the present study for the estimation of the ripening stage of apples of Fuji variety.

2.1. Data collection

The first step of the research process is to collect apple samples for the prediction of their ripening state. For this purpose, a total of 172 samples of apples (*Malus domestica* L. var. Fuji) were collected in four different stages (43 samples per stage) from an orchard in Kermanshah, Iran (34.3277° N, 47.0778° E). Before data collection, the most precise ripening date of the apples was determined by expert human gardeners. Then, for the purpose of the present study, we decided to collect the samples at 7-day intervals before and after the given ripening date. Specifically, the first stage of harvest was 14 days before ripening, the second was 7 days before ripening, the third on the ripening date, and finally the fourth was 7 days after ripening. Thus, there is a period of one week between the four harvest stages. In this paper, the stages 1-4 are named as unripe, half-ripe, ripe and over-ripe, respectively.

2.2. Spectroscopy of the samples

After obtaining the samples, the second step is to extract the spectral information from each apple sample, trying to minimize the noise of the signals. This step is divided into two main parts: spectral data extraction, and spectral enhancement. Obviously, the spectroscopy is done just after each of the four harvest stages for the corresponding samples.

2.2.1. Extraction of spectral data from the samples

The hardware system used to perform the spectral analysis consists of four main components, including the spectrometer, a light source, an optical fiber and a laptop PC. The laptop was used to store the obtained spectral data using SpectraWiz software (StellarNet Inc., Tampa, Florida, USA). The spectrometer was a model EPP200NIR (StellarNet Inc., Tampa, Florida, USA) adjusted to capture the spectral reflectance in the range from 450 to 1000 nm, thus including visible light (450-750 nm) and a part of the near-infrared (750-1000 nm). The detector embedded was indium-gallium-arsenide. The light source was a tungsten halogen lamp with 20W (StellarNet Inc., Tampa, Florida, USA). Two plug-in optical fibers were used for transmitting light from the light source to the samples, and from the samples to the spectrometer. For each sample, a total of 1943 wavelengths were captured, with an average width of 0.28 nm for each captured band.

2.2.2. Spectral enhancement

Due to different reasons such as the effect of ambient light, the spherical surface of the apples, the properties of the spectrometer used, and the type of light source, the spectral data extracted have some noise that should be reduced before using it. The preprocessing of the signals consists of three steps: converting reflection to absorption spectra; light scatter and baseline corrections; and signal smoothing. In the first step, the conversion of the obtained reflectance spectra into absorption spectra is done using the following equation:

$$Absorption_s(w) = \log_e \left({}^{1}/_{Reflectance_s(w)} \right) \quad (1)$$

where s is the number of the apple sample (from 1 to 172), and w is the wavelength considered (from 450 to 1000 nm).

The second stage is light scatter and baseline corrections by wavelet detrending algorithm (Rossel, 2008), whose purpose is to obtain a correct normalization of the signals. Basically, this method consists in applying the discrete wavelet transform (DWT) to the spectrum using a Daubechies wavelet with 4 vanishing moments. In order to detrend the signal, the components with lower frequency are removed. So, the signal is reconstructed using only the components with higher frequency, i.e. those that change more quickly. Finally, the third step is smoothing the signals, which is done applying the median filter algorithm. After this preprocessing, it was observed that 3 apple spectra had non-standard graphs as compared to the rest of samples. In other words, the spectral graphs obtained from these 3 samples were considerably different in shape from the others. According to Nicolaï et al. (2007) the spectral graphs of the same fruits are similar; therefore, these 3 samples were removed from the experiments since the could be due to an error in the system or in the capture process.

2.3. Extraction of color features of the samples

The color model CIE L*a*b* has proved to be one of the most comprehensive and useful for industrial applications in general, and specifically for computer vision in agriculture (Cardenas-Perez et al., 2017; Hernández-Hernández et al., 2017; García-Mateos et al., 2015). For this reason, this model has been used in the present work in order to extract color information from the apple samples. In particular, the L*, a* and b* components of each sample were measured with a CR-400 colorimeter (Konica Minolta, Tokyo, Japan). Then, the parameter called hue angle, h_a, proposed by (Clerici et al., 2011) for agricultural applications, was calculated as follows:

$$h_a = \tan^{-1}\left(b^* / a^*\right) \tag{2}$$

By computing the arctangent of the a* and b* channels, this equation achieves a more robust way to obtain the hue angle than the traditional H channels in HSV and HLS color spaces. On the other hand, the combination of channel b* and h_a has shown to be a powerful set of color features for apple image processing. Thus, both parameters will be considered as the input for the ripeness estimation based on color features.

2.4. Ripeness estimation using an ensemble of classifiers

This subsection describes the proposed classification method based on a combination of five classifiers that are combined with the majority voting rule. First, the individual classifiers are presented, and then the combination process is introduced. This method is applied both to the color features and to the spectral information of the selected bands.

2.4.1. Hybrid artificial neural network – genetic algorithm (ANN-GA)

Genetic algorithm is one of the most powerful optimization methods inspired by the nature of organisms. This algorithm is based on the principles of natural evolution. As a general rule, in nature only powerful animals win the competition over food and are, therefore, capable of generating. This superiority is due to their individual characteristics, expressed in their genes. With reproduction, these genes proliferate and produce better offspring. Therefore, by sequentially selecting the best population and reproducing through them, there will be a population with greater ability to adapt to the environment, resulting in better and more resource-efficient community members (Garg, 2016).

In this way, the hyperparameters of the ANN are selected as a vector for the genetic algorithm (GA), which controls the execution of the ANN. The performance of each run of the ANN is recorded by the GA using the mean squared error (MSE) of the test set. In this case, the inputs of the ANN are spectral data, and the outputs are the corresponding classes (unripe, half-ripe, ripe and over-ripe). Finally, set of hyperparameters of the ANN with the least MSE is selected as the optimal structure by the GA.

The number of layers selectable by the genetic algorithm was set between 1 and 3. The number of neurons selectable for the first layer was between 1 and 25, for the rest of layers between 0 and 25 (a 0 means that the layer is not used). The possible transfer functions, back propagation-network training functions, and the weight/bias-back propagation learning functions were selected from the Neural Network Toolbox of MATLAB software (MathWorks, Natick, MA, USA). After adjusting the hyperparameters of the ANN, the reliability of the ANN was evaluated using 1000 iterations. It should be noted that 60% of data were randomly selected for training, 10% for validation, and the remaining 30% for test. These proportions are used in all the classifiers. Each repetition involves a different selection of the training/validation/test sets and a different random initialization of the weights of the ANN.

2.4.2. Hybrid artificial neural network – particle swarm optimization (ANN-PSO)

The particle swarm optimization (PSO) algorithm is another meta-heuristic algorithm that mimics the mass movements of birds to optimize different problems. This algorithm was first proposed by Kennedy and Eberhat (1995). Each answer to the problem is considered a particle. Every single particle is constantly searching and moving. The motion of each particle depends on three factors: (1) the current position of the particle; (2) the best position the particle has ever had; and (3) the best position the entire set of particles has ever had. The application of this hybrid method is similar to the procedure described for ANN-GA. In this way, PSO controls the execution of the ANN using different sets of hyperparameters, selecting the optimal configuration.

2.4.3. Hybrid artificial neural network – firefly algorithm (ANN-FA)

The main idea of the firefly algorithm (FA) is inspired by the flashing behavior of fireflies. This algorithm can be seen as an expression of swarm intelligence in which the cooperation (and possibly competition) of simple, low-intelligence members results in a higher level of intelligence that is certainly not attainable by any component (Yang, 2009). Again, this metaheuristic algorithm is used to obtain the optimal set of hyperparameters of the ANN, performing different executions controlled by the FA, and selecting the setup with least MSE.

2.4.4. Support vector machine (SVM)

Support vector machines are one of the most popular supervised learning methods that are used for classification and regression. This method performs the sorting operation using linear data categorization (Cortes and Vapnik, 1995). Using a kernel function, this classifier implicitly maps the input data into a high-dimensional space, resulting in nonlinear decision boundaries. In the present study, the kernel function was a simple dot product. The soft margin parameter (C) value was considered as 1. These values were selected by trial and error using a given dataset. The kernel functions considered are dot product, polynomial, radial basis function (RBF) and sigmoid.

2.4.5. k-nearest neighbors (kNN)

The k-nearest neighbor algorithm is a non-parametric method that can be used for classification or regression. This method classifies each new sample based on the closest properties of other elements in its neighborhood. In general, this method works as follows:

- Determine the number of neighbors near the input sample to consider, i.e. parameter k.
- Calculate the distance of the input sample with all the training samples. This distance is usually measured in terms of the Euclidean distance. Assuming two n dimensional tuples, $x = (x_1, x_2 \ldots x_n)$ and $y = (y_1, y_2 \ldots y_n)$, then the Euclidean distance between these two sets is calculated with:

$$D(x, y) = \sqrt{\sum_{i=1}^{n} (x_i - y_i)^2} \tag{3}$$

- Sort the training samples in increasing order of the distance to the input sample.
- The class with the highest number of training samples between the k nearest neighbors is selected as the estimated class of the input sample (Bhuvaneswari & Therese, 2015).

In this paper, after executing different trials and errors, it was found that the neighborhood number 11 (k = 11) achieved the highest classification accuracy. So, this is the value used in the experiments.

2.4.6. Majority-Voting Ensemble (MV)

Since ensemble decision making is more reliable than individual decisions, the proposed approach consists in the application of the five presented classifiers (ANN-GA, ANN-PSO, SVM and kNN) combined with the majority voting method. That is, given an input sample, each classifier votes for one class, and then the class with the highest number of votes is selected as the predicted output. One of the most important advantages of the MV method is to avoid overfitting of the training model, since the risk is overfitting would only appear if most of the constituent methods overfitted the training samples.

2.5. Ripeness estimation using classical ANN

In order to compare the accuracy of the proposed ensemble approach, an alternative classifier was developed following a classical ANN scheme, whose hyperparameters are selected by grid search. The ANN applied in this study is a standard feed-forward, back-propagation neural network. In this case, the input of the ANN is the complete spectral information from 450 to 1000 nm; and the output is the corresponding ripening class (unripe, half-ripe, ripe and over-ripe). By taking a different input is this method, the experimental results can be used to observe the effectivity of using the full spectrum of the samples or only a narrow band.

Basically, the grid search of the hyperparameters consists of defining the possible values for each parameter, executing the training process of the ANN for all the combinations, and selecting the

ANN structure with the least MSE. In this way, the grid search is a more complete procedure than the metaheuristic methods, since it tests all the possible combinations of the hyperparameters; however, the possible values of each parameter have to be reduced to avoid exponential growth in runtime.

In our case, the possible number of neurons for each hidden layer was fixed to 5 or 10. The number of hidden layers was between 1 and 10. The transfer functions, the back propagation-network training functions, and the weight/bias-back propagation learning functions were also selected from the Neural Network Toolbox of MATLAB software (MathWorks, Natick, MA, USA). After obtaining the optimal set of hyperparameters of the ANN, the accuracy of the classification was also evaluated through 1000 iterations. As in the proposed ensemble, data samples were randomly divided into three disjoint sets. The first set contains 60% of the data samples for training, the second contains 10% of the data for validation, and the third contains the remaining 30% for testing,

2.6. Measures for evaluating the performance of the classifiers

Different common criteria are used to evaluate the performance obtained by the proposed classifiers. The first category is the confusion matrix (i.e. the number of test samples according to the expected and the obtained class), and the measures that are computed from it: recall, accuracy, specificity, precision, and F-measure. The second category of performance measures is the plot of the receiver operating characteristic (ROC) curve, as well as the area under the ROC curve defined from it (Sabzi & Abbaspour -Gilandeh, 2018; Sabzi et al., 2018; Pourdarbani et al., 2019).

3. Result and Discussion

3.1. Preprocessed spectral graphs

The first interesting aspect to analyze from the experimental results is the effectivity of the preprocessing step. Fig. 2 shows a comparison of the plots of the reflectance spectra and the preprocessed spectra of the different apple samples.

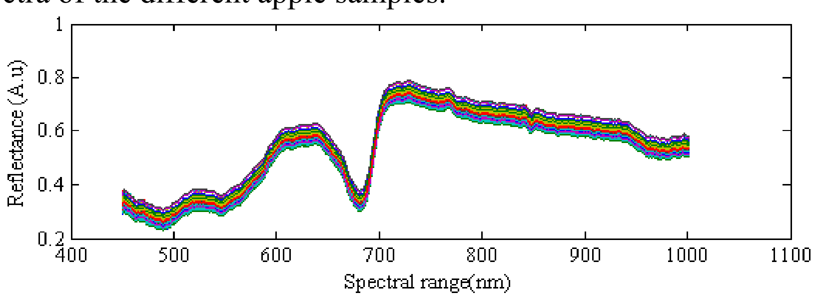

(a)

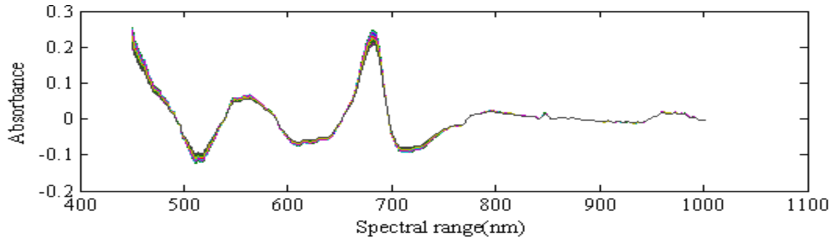

(b)

Fig. 2. Spectral graphs of different samples of Fuji apple. (a) Reflectance spectrum. (b) Preprocessed absorption spectrum.

There is an evident inversion effect, since Fig. 2a represents reflectance and Fig. 2b represents absorption. Besides, the normalization and smoothing processes greatly reduce the variability of the original signals. Nevertheless, as can be observed, the preprocessed graphs have different fine and coarse peaks, each of which has specific information of interest. For this reason, the information in three spectral bands of 465 to 485 nm, 675 to 700 nm and 870 to 890 nm was used to classify the different ripening stages of Fuji apples.

3.2. Optimal structure of the ANN classifier

Table 1 presents the optimal hyperparameters of the ANN classifier obtained in the grid search procedure. Recall that this method uses all the spectral information of each sample.

Number of hidden layers	Number of neurons	Transfer function	Backpropagation network training function	Backpropagation weight/bias learning function
1	10	logsig	trainscg	learnp

Table 1. Optimal structure of the hyperparameters of the classical ANN. logsig: log-sigmoid transfer function. trainscg: scaled conjugate gradient backpropagation. learnp: perceptron weight and bias learning function.

Surprisingly, although the grid search tested complex ANN structures with up to 10 hidden layers, the optimal configuration for the ANN method is using only one hidden layer, which contains 10 neurons. This fact can be explained by the shape of the decision boundaries and the relatively small number of training samples, which favors a simple structure over a deeper one.

3.3. Optimal structure of the ANNs adjusted by metaheuristics

In the case of the hybrid methods, the hyperparameters of the ANN are adjusted by means of the execution of the three proposed metaheuristic algorithms, as explained in section 2. Table 2 contains the optimal structure of the hidden layers of the ANNs adjusted with GA, FA and PSO algorithms.

Method	Number of hidden layers	Number of neurons	Transfer function	Backpropagation network training function	Backpropagation weight/bias learning function
ANN-GA	2	1st layer: 18	1st layer: tribas	traingd	learnp
		2nd layer: 5	2nd layer: hardlims		

ANN-FA	2	1st layer: 7	1st layer: satlin	traincgf	learnsom
		2nd layer:16	2nd layer: tansig		
ANN-PSO	3	1st layer: 11	1st layer: hardlims	traingd	learnhd
		2nd layer:19	2nd layer: purelin		
		3rd layer: 6	3rd layer: logsig		

Table 2. Hyperparameters of the ANNs adjusted by different algorithms. GA: genetic algorithm. FA: firefly algorithm. PSO: particle swarm optimization. tribas: triangular basis. hardlims: symmetric hard-limit. satlin: saturating linear. tansig: hyperbolic tangent sigmoid. purelin: linear. logsig: log-sigmoid. traingd: gradient descent. traincgf: scaled conjugate gradient. learnp: perceptron weight and bias. learnsom: self-organizing learning map. learnhd: Hebb with decay weight learning rule.

The ANN structures obtained by the different hybrid methods are very varied, even though they used the same datasets. In this case, unlike the result obtained by the grid search, the optimal number of hidden layers ranges from 2 to 3. The number of neurons per layer is also very varied, going from 5 to 19. This large variability is also in the selection of the transfer and backpropagation functions.

3.4. Ripeness estimation using color features

The proposed ensemble classifier was applied using the extracted color features, b* channel and hue angle h_a. Table 3 presents the obtained confusion matrix, the error rates per class, and the correct classification rate (CCR), performing 1000 repetitions of the training/test process. Since there are 164 apple samples, 30% of them (49 apples) were used for the test in each repetition. Thus, the total number of test samples is equivalent to 49000 samples.

Real/estimated class	Unripe	Half-ripe	Ripe	Over-ripe	Total data	Classification error per class (%)	Correct classification rate (%)
Unripe	10604	291	0	0	10895	2.67	95.12
Half-ripe	386	11012	201	12	11611	5.16	
Ripe	5	59	13103	538	13705	4.39	
Over-ripe	2	2	893	11892	12789	7.01	

Table 3. Confusion matrix and accuracy measures obtained by the MV method for the prediction of the ripening state of Fuji apples using input color features (b* and h_a) with 1000 iterations.

As shown in Table 3, among the 49000 test samples, only 2389 were incorrectly classified, thus resulting in a CCR of 95.12%. Table 4 contains the five criteria for the performance evaluation for this experiment. Since the recall criterion indicates the percentage of correctly identified samples, it can be understood that more than 96% of the samples are correctly identified for the unripe and half-ripe classes.

Class	Recall (%)	Accuracy (%)	Specificity (%)	Precision (%)	F-measure (%)

Unripe	96.43	98.55	99.19	97.33	96.87
Half-ripe	96.90	98.00	98.34	94.84	95.86
Ripe	92.29	96.49	98.23	95.61	93.92
Over-ripe	95.58	96.99	97.48	92.99	94.26

Table 4. Performance evaluation criteria obtained by the MV method for the prediction of the ripening state of Fuji apples using input color features (b* and h_a) with 1000 iterations.

As can be seen in Table 4, the highest accuracy is related to the classes unripe and half-ripe. The specificity of 100% means that samples of classes other than the target class are correctly identified. The obtained specificities over 98% indicate high performance of the classification for classes unripe, half-ripe, ripe and over-ripe. A precision of 100% in each class means that none of the samples are incorrectly classified in another class. In this case, Table 3 indicates that only in unripe class the precision is over 97%, so a low number of the samples of unripe class are classified into another class. Finally, the last column of Table 3, the F-measure, is obtained using the criteria of precision and recall. In fact, the F-measure is a harmonic weighted average of these two criteria. Fig. 3 shows the box diagrams of the two main criteria for evaluating the performance of MV method using color features. It was observed that only 13 iterations of the training/test process produced a CCR below 90%, with two of them below 50%. In general, the obtained box plots indicate the high repeatability of the MV method proposed in this paper.

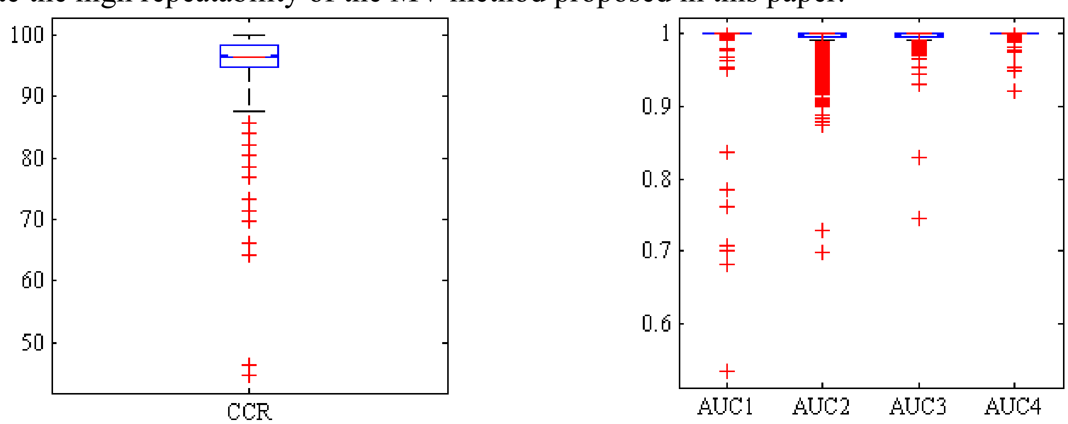

(a) (b)

Fig. 3. Box diagrams of two criteria for evaluating the performance of the MV method using b* and h_a, with 1000 iterations. (a) Correct classification rate. (b) Area under the ROC curves (AUC) for the classes unripe (AUC1), ripe (AUC2), half-ripe (AUC3) and over-ripe (AUC4).

3.5. Ripeness estimation using spectral data

3.5.1. Spectral range from 450 to 1000 nm

As mentioned in section 2, the ANN adjusted with the grid search was executed using the full spectra of the samples, in the wavelengths from 450 to 1000 nm, which includes visible light and a part of the near-infrared. Table 5 shows the confusion matrix and the accuracy measures (CCR) of this model after the 1000 repetitions. As can be seen, 3857 samples were incorrectly classified, resulting in a CCR of 92.12%. The highest classification error of this method was produced for the unripe class, with 17.71% error. The predefined performance measures are presented in Table 6.

Real/estimated class	Unripe	Half-ripe	Ripe	Over-ripe	Total data	Classification error per class (%)	Correct classification rate (%)
Unripe	10059	126	1566	473	12224	17.71	92.12
Half-ripe	59	11916	5	145	12125	1.72	
Ripe	333	13	11512	476	12334	6.67	
Over-ripe	5	101	555	11656	12317	5.36	

Table 5. Confusion matrix and accuracy measures obtained by the ANN method adjusted with grid search, for the prediction of the ripening state of Fuji apples using spectral range 450-1000 nm, with 1000 iterations.

Class	Recall (%)	Accuracy (%)	Specificity (%)	Precision (%)	F-measure (%)
Unripe	82.29	95.78	99.18	96.20	88.70
Half-ripe	98.28	99.14	99.34	98.03	98.15
Ripe	93.34	93.98	94.20	84.41	88.64
Over-ripe	94.63	96.41	97.01	91.22	93.00

Table 6. Performance evaluation criteria obtained by the ANN method adjusted with grid search, for the prediction of the ripening state of Fuji apples using spectral range 450-1000 nm, with 1000 iterations.

In this case, the error is not only bigger than that obtained by the ensemble classifier using color, but it also produces larger error in classes separated by more than one stage. For example, while only 5 samples of the ripe class were misclassified as half-ripe, more than 1500 ripe apples were predicted as unripe; and 473 over-ripe apples were misclassified as unripe. This problem was not observed in the classification using color, where most errors were in the range of one stage.

Fig. 4 shows a box-diagram of the two criteria, namely CCR and AUC, for the 1000 iterations. The graph of CCR shows that only 14 iterations have a value of less than 70%, although most of them are above 90%. The values of AUC present a large diversity, which shows that this method is not so stable.

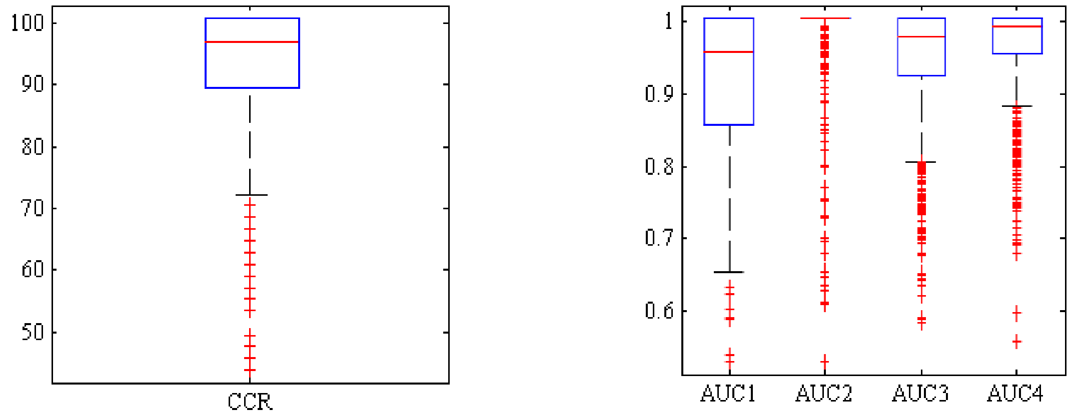

(a) (b)

Fig. 4. Box diagrams of two criteria for evaluating the performance of the ANN method adjusted with grid search, with 1000 iterations. (a) Correct classification rate. (b) Area under the ROC curves (AUC) for the classes unripe (AUC1), ripe (AUC2), half-ripe (AUC3) and over-ripe (AUC4).

3.5.2. Spectral range from 465 to 485 nm

The first spectral range analyzed is located in the wavelengths from 465 to 485 nm, which roughly corresponds to the blue-cyan colors. Table 7 indicates the obtained performance of the ensemble classifier with the MV method using this spectral data, including the confusion matrix, the classification errors per class and the total CCR.

Real/estimated class	Unripe	Half-ripe	Ripe	Over-ripe	Total data	Classification error per class (%)	Correct classification rate (%)
Unripe	10798	37	0	30	10865	0.617	99.37
Half-ripe	40	11716	0	18	11784	0.492	
Ripe	0	79	13201	90	13370	1.260	
Over-ripe	4	1	7	12696	12981	0.092	

Table 7. Confusion matrix and accuracy measures obtained by the ensemble classifier with MV method, for the prediction of the ripening state of Fuji apples using spectral range 465-485 nm, with 1000 iterations.

In this case, the confusion matrix is more similar to an ideal identity matrix, showing that this method is more effective than the previous alternatives. The highest classification error is related to the ripe class, but it is only a 1.26% error. The obtained CCR above 99.3% proves that it has been able to classify the samples in their correct classes, indicating a very high performance. Table 8 represents the measures of this method for the 1000 random iterations using the measures obtained from the confusion matrix.

Class	Recall (%)	Accuracy (%)	Specificity (%)	Precision (%)	F-measure (%)
Unripe	99.59	99.77	99.82	99.38	99.49
Half-ripe	99.01	99.64	99.84	99.51	99.26

Ripe	99.95	99.63	99.83	98.74	99.34
Over-ripe	98.95	99.69	99.97	99.91	99.42

Table 8. Performance evaluation criteria obtained by the ensemble classifier with MV method, for the prediction of the ripening state of Fuji apples using spectral range 465-485 nm, with 1000 iterations.

According to Table 8, in all the cases (except for the precision of the ripe class), the criteria are higher than 99%, indicating the very high performance achieved. Fig. 5 confirms the results of Tables 7 and 8 using box diagrams of the AUCs and CCR after the 1000 repetitions. This figure shows that only in 16 iterations the CCR fell below 100%, probably due to a very unbalanced selection of the training/validation/test samples for those iterations. The same effect can be observed in the AUC values (Fig. 5b), which are almost always very close to 1, except for some sparse executions. Only about 1.5 % of the iterations have results below 1 for these performance measures.

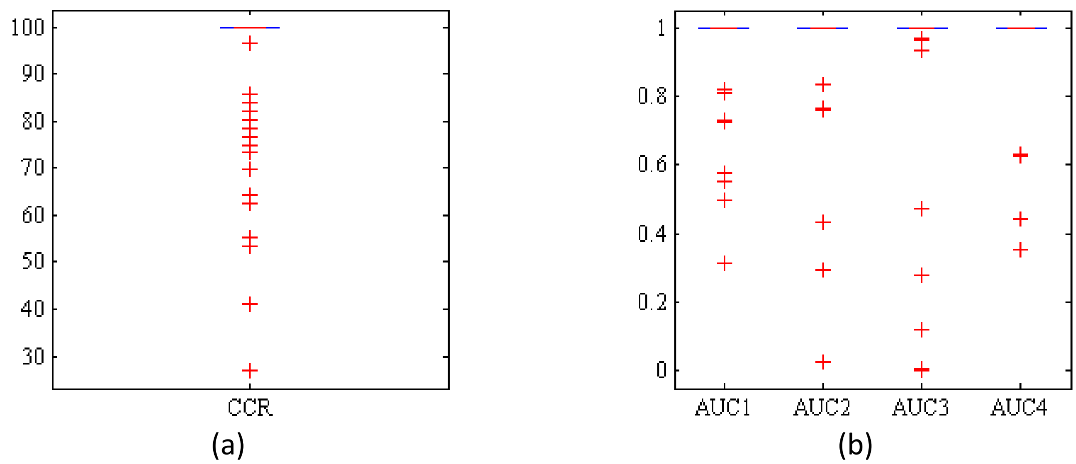

Fig. 5. Box diagrams of two criteria for evaluating the performance of the ensemble classifier with MV method, with 1000 iterations using spectral range 465-485 nm. (a) Correct classification rate. (b) Area under the ROC curves (AUC) for the four ripening classes.

3.5.3. Spectral range from 675 to 700 nm

The second spectral range selected corresponds to the wavelengths from 675 to 700 nm, which belong to the red color as observed by the human visual system. Tables 9 and 10, and Fig. 6 present the main results from the experiments for this range, indicating the confusion matrix, the performance criteria and the box plot of the measures, respectively.

Real/estimated class	**Unripe**	**Half-ripe**	**Ripe**	**Over-ripe**	**Total data**	**Classification error per class (%)**	**Correct classification rate (%)**
Unripe	10342	463	13	11	10829	4.49	97.56
Half-ripe	596	11115	15	20	11746	5.37	
Ripe	4	30	13428	43	13505	0.57	
Over-ripe	0	0	0	12920	12920	0.00	

Table 9. Confusion matrix and accuracy measures obtained by the ensemble classifier with MV method, for the prediction of the ripening state of Fuji apples using spectral range 675-700 nm, with 1000 iterations.

Class	Recall (%)	Accuracy (%)	Specificity (%)	Precision (%)	F-measure (%)
Unripe	94.51	97.78	98.72	95.50	95.00
Half-ripe	95.75	97.70	98.31	94.63	95.19
Ripe	99.79	99.78	99.78	99.43	99.61
Over-ripe	99.43	99.84	100	100	99.71

Table 10. Performance evaluation criteria obtained by the ensemble classifier with MV method, for the prediction of the ripening state of Fuji apples using spectral range 675-700 nm, with 1000 iterations.

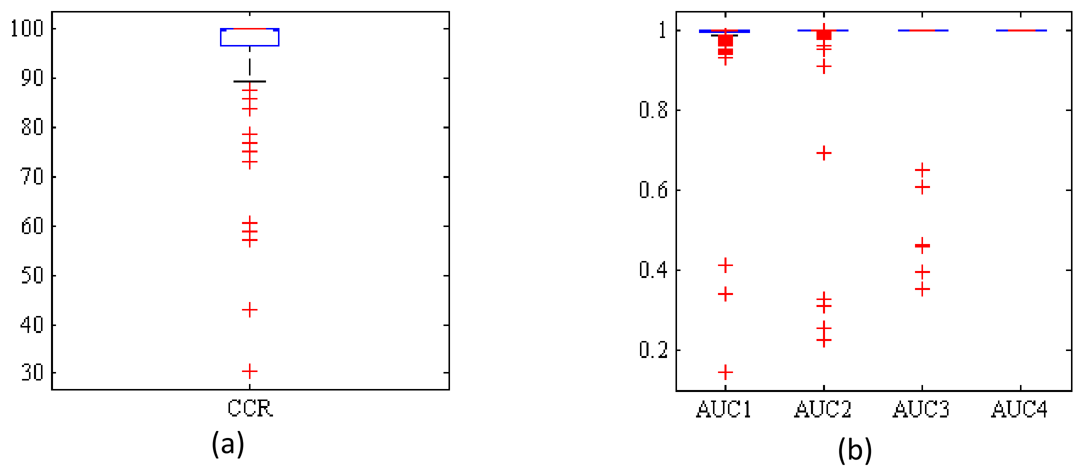

Fig. 6. Box diagrams of two criteria for evaluating the performance of the ensemble classifier with MV method, with 1000 iterations using spectral range 675-700 nm. (a) Correct classification rate. (b) Area under the ROC curves (AUC) for the four ripening classes.

This experiment shows that the effectivity of the range from 675-700 nm is significantly lower than that of the range 465-485 nm. The obtained CCR is over 97.5%, which is 2% less than the previous case. While, the classification of the over-ripe samples was perfect, the errors in the unripe and half-ripe classes are very large, 4.49% and 5.37%, respectively. This result may seem surprising, since a ripe Fuji apple is characterized by a bright red color. However, the experiments show that just using the red color wavelengths is not enough to discriminate to ripening stage. Yet, the obtained accuracy is considerably higher than those obtained with color features (95%) and using all the VIS-NIR spectrum (92%). Another interesting result is that the box plots (Fig. 6) indicate that the method is very stable.

3.5. Spectral range from 870 to 890 nm

The third spectral range selected, from 870 to 890 nm, is located in the lower part of the infrared wavelengths, known as the near-infrared. This radiation is not visible by the human eye, but it contains information of interest for many applications in agriculture. Table 11 contains the resulting confusion matrix, classification errors per class and CCR, Table 12 the five performance criteria, and Fig. 7 the corresponding box plots.

Real/estimated class	Unripe	Half-ripe	Ripe	Over-ripe	Total data	Classification error per class (%)	Correct classification rate (%)
Unripe	10303	419	14	20	10756	4.21	97.80
Half-ripe	388	11161	140	22	11711	4.69	
Ripe	0	22	13473	40	13535	0.46	
Over-ripe	0	0	12	12986	12998	0.09	

Table 11. Confusion matrix and accuracy measures obtained by the ensemble classifier with MV method, for the prediction of the ripening state of Fuji apples using spectral range 870-890 nm, with 1000 iterations.

Class	Recall (%)	Accuracy (%)	Specificity (%)	Precision (%)	F-measure (%)
Unripe	96.37	98.27	98.81	95.79	96.08
Half-ripe	96.19	97.97	98.52	95.30	95.75
Ripe	98.78	99.53	99.82	99.54	99.16
Over-ripe	99.37	99.80	99.96	99.91	99.64

Table 12. Performance evaluation criteria obtained by the ensemble classifier with MV method, for the prediction of the ripening state of Fuji apples using spectral range 870-890 nm, with 1000 iterations.

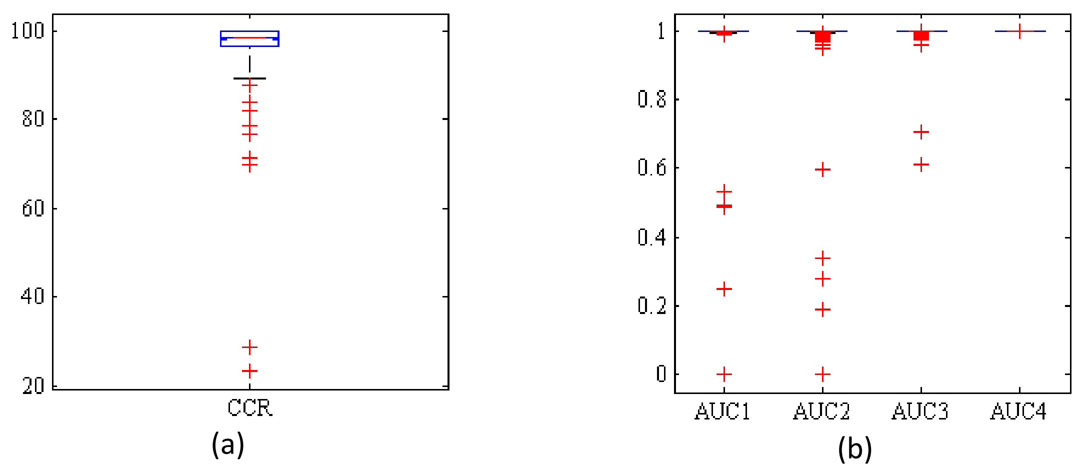

Fig. 7. Box diagrams of two criteria for evaluating the performance of the ensemble classifier with MV method, with 1000 iterations using spectral range 870-890 nm. (a) Correct classification rate. (b) Area under the ROC curves (AUC) for the four ripening classes.

As can be seen, only 1077 from the 49000 samples of the test set were incorrectly classified, resulting in CCR of 97.80%. These results are very similar to the case of 675-700 nm, with a CCR of 97.56%. Moreover, a very similar distribution of the errors is observed, with the ripe and over-ripe classes below 0.5% error, while unripe and half-ripe errors are above 4%. Similarly, the box plots prove that this case is also very stable. For example, only 10 iterations produced a CCR below 90%, and most performance criteria are close to 1.

3.6. Comparison of classifiers using color data and spectral data

After analyzing each of the models individually, this subsection compares the experimental results of all the models and the constituent members of the ensemble classifiers. This can offer us a more detailed view of the advantages and disadvantages of each choice.

In the previous subsections, the results of the ensemble classifier for the four different types of input have been presented. Table 13 shows the classification accuracy obtained by the basic classifiers contained in each ensemble model for the four input types.

Basic classifier	Color b*, h_a	Spectral data 465 to 485 nm	Spectral data 675 to 700 nm	Spectral data 870 to 890 nm
ANN-GA	95.06	93.12	87.41	94.28
ANN-PSO	95.88	91.07	95.92	93.69
ANN-FA	97.16	99.31	93.99	97.72
SVM	93.67	73.71	90.42	97.51
kNN	92.56	98.79	89.76	97.52

Table 13. Results obtained by the five basic classifiers that make up the ensemble classifier for the four types of input data (color information or narrow spectral bands). The values indicate the mean correct classification rate (CCR) of each method after the 1000 repetitions.

It can be concluded that there is no single classifier that achieves the best accuracy in all cases. ANN-FA is the most effective model in 3 of the 4 cases, but it fails to produce a high accuracy using the spectral band from 675 to 700 nm. In that case, the best basic method is ANN-PSO. Regarding the classifiers that are not based on ANN, they have an irregular behavior, in some cases below the accuracies of the ANN models and in other cases above them. kNN is close to the optimum in the 465-485 nm band, and both SVM and kNN are above 97.5% CCR for the 870-890 nm band. However, SVM produces poor results for the 465-485 nm band of only 73.7%, and kNN only 89.8% for the spectral data in 675 to 700 nm.

Table 14 contains the mean and standard deviation (SD) of the CCR and AUC values for the 1000 iterations of the training/test process, and also the values for the best iteration. Compared to the results of the basic classifiers presented in Table 13, the ensemble method is able to improve these results in all the cases, except using color information (where ANN-FA achieves 97.16% CCR and the ensemble only 95.12%); since the input tuples only have 2 values in this case, the capability of the combination to improve the constituent methods is very reduced. However, in the rest of cases, containing larger input tuples, the benefits are more evident. For example, in the spectral band from 675 to 700 nm, the basic methods are below 95.9% accuracy, while the ensemble achieves a mean CCR of 97.56%.

Method	Input data	Iteration	CCR (%)	AUC1	AUC2	AUC3	AUC4

Ensemble with MV	Color b*, h_a	Mean	95.12	0.998	0.989	0.997	0.999
		SD	4.92	0.025	0.027	0.012	0.004
		Best training	100	1	1	1	1
	Spectral data 465 to 485nm	Mean	99.37	0.997	0.997	0.989	0.998
		SD	5.17	0.036	0.043	0.097	0.031
		Best training	100	1	1	1	1
	Spectral data 675 to 700nm	Mean	97.56	0. 994	0.995	0.997	1
		SD	4.85	0.039	0.047	0.040	0
		Best training	100	1	1	1	1
	Spectral data 870 to 890nm	Mean	97.80	0.995	0.994	0.999	0.999
		SD	4.40	0.057	0.053	0.016	0.003
		Best training	100	1	1	1	1
ANN	Spectral data 450 to 1000nm	Mean	92.12	0.908	0.98	0.93	0.95
		SD	6.88	0.099	0.046	0.083	0.06
		Best training	100	1	1	1	1

Table 14. Correct classification rates (CCR) and area under the ROC curves (AUC) for the four ripening classes, for the 1000 repetitions of each case, and for all the models analyzed in the experiments, considering the mean, standard deviation (SD) and best execution.

According to Table 14, all the methods were able to achieve a perfect classification (CCR 100% and AUC values 1) in the best repetition of the training/test process. However, the most interesting parameters are relative to the mean and SD values. In general, all the methods have an average CCR above 92%. However, the option of using all the spectral range available proves to be worse than using also a narrow band; it is 7% worse than selecting the optimal band of 465-485 nm, considering the CCR. This effect can also be due to the use of a different classifier, since the classification with narrow bands is done with the ensemble classifier, while the full spectrum is classified with an ANN adjusted with grid search. Although the ensemble classifier could also be applied to the full spectrum, some of its constituent methods, such as SVM and kNN, are not adequate for the high dimensionality of the input tuples and the small number of samples available. For this reason, this input was only classified with an ANN specifically optimized for those conditions. On the other hand, the use of color information is not able to reach the high levels of accuracy of spectral data. It must be noted than some of these narrow bands actually correspond to visible light (e.g. the optimal band 465-485 nm are blue colors). But the use of this narrow band spectrography offers, in our case, about 70 values for each input tuple, while the colorimetry values are only 2 (b* and h_a).

Fig. 8 shows the ROC curves for the five proposed methods for each ripening class. These graphs confirm again the positive results of the proposed method, with a close to ideal plot for the optimal color. Thus, the proposed method can be easily configured to produce a small number of false positives and false negatives.

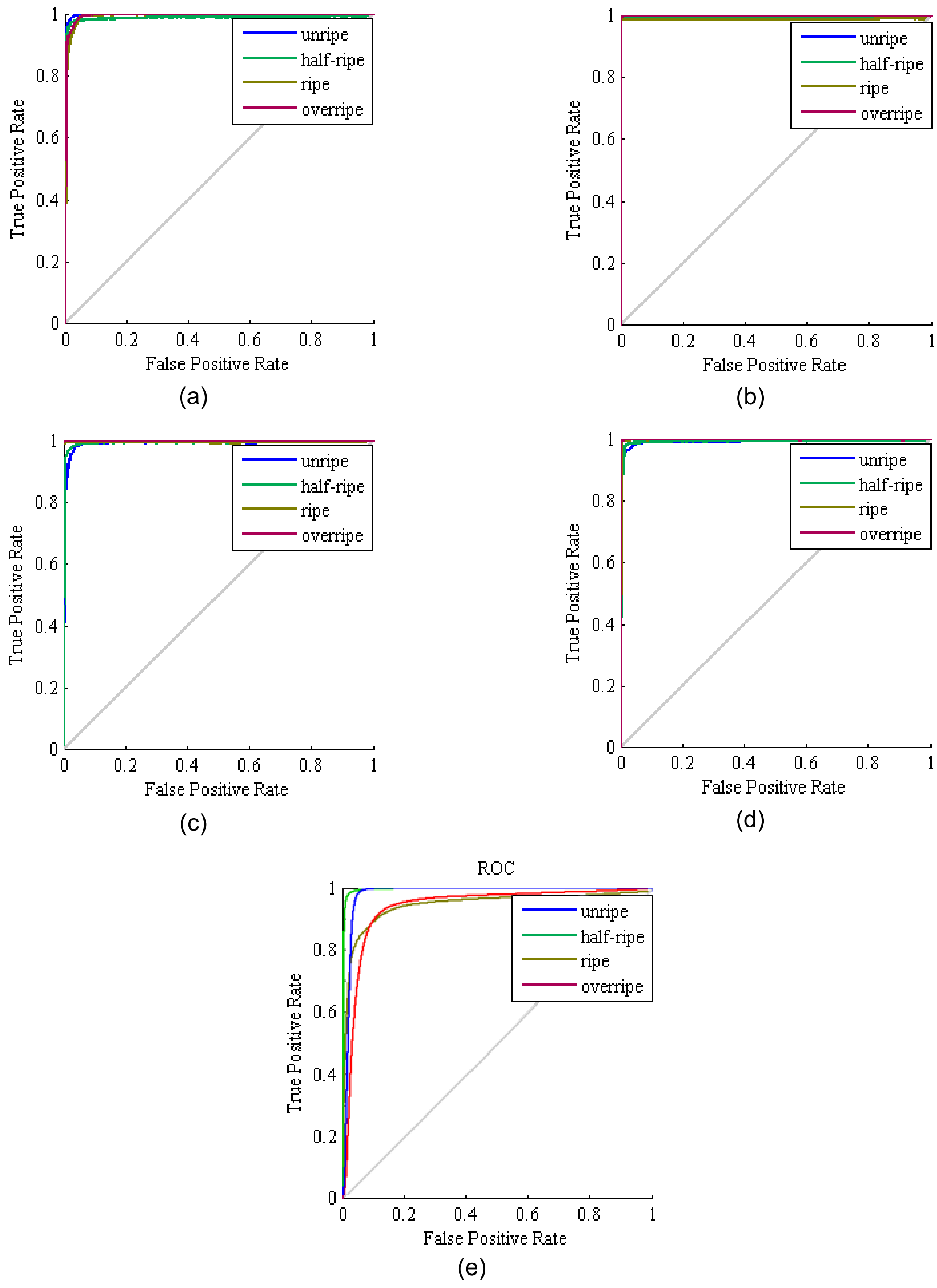

Fig. 8. Receiver operating characteristic curves (ROC) of the five proposed models for the estimation of the ripening stage is Fuji apples for the 1000 repetitions. (a) Ensemble classifier using color features, b* and ha. (b) Ensemble classifier using spectral range 465-485 nm. (c) Ensemble classifier using spectral range 675-700 nm. (d) Ensemble classifier using spectral range 870-890 nm. (e) ANN classifier using spectral range 450-1000 nm.

3.6. Comparison of the proposed method and previous works

After presenting the performance of the proposed algorithm for determining the ripening stages using different criteria, in this subsection the results are compared with the techniques proposed by other researchers in the state of the art. The most similar works to our case (in terms of objectives and methodology) have been selected, although these studies are different in the specific domain and the datasets applied. Thus, the comparison should only be considered in a very generic way, since a direct comparison is not possible.

Table 15 shows the CCR values reported in the selected previous papers. In the case of (Tian et al., 2019), they conducted a study on apples to identify different ripening stages using color data. The results reported a CCR of 89.60%. Adebayo et al. (2016) investigated ripening stage of banana fruits using spectral data below 1000 nm. A total of 320 samples were tested. The results showed a CCR of 97.53%, which is comparable to some of our narrow band models. Finally, Mohammadi et al. (2015) carried out a study on ripening of persimmon fruits using different color features such as the first and second channels of RGB color space, and third channel of CIE L*a*b*. In this case, the CCR of their method was 90.24%.

CCR (%)	Method	Fruit	Researcher
95.12	Color features	Apple	Proposed method
99.37	Narrow spectral bands	Apple	Proposed method
92.12	Wide spectral band	Apple	Proposed method
89.60	Color features	Apple	(Tian et al., 2019)
97.53	Spectral features	Banana	(Adebayo et al., 2016)
90.24	Color features	Persimmon	(Mohammadi et al., 2015)

Table 15. Comparison of the results of present study with the results of other researchers to identify different stages of fruit ripening.

As mentioned, a direct comparison is not feasible, since the datasets and the capture conditions are nor equivalent. In any case, it can be observed that the proposed method is able to achieve a very precise result in the context of the state of the art, with a CCR over 99%.

4. Conclusion

In this paper, a new algorithm for the estimation of the ripening stage of Fuji apples based on color features and narrow spectral bands has been presented. The obtained information is in the wavelengths from 450 to 1000 nm, corresponding to visible light and near infrared. The color features are extracted from the CIE L*a*b* color space, including the b* channel and the hue angle.

To achieve an effective classification, a new ensemble classification method has been proposed, where the results of the five constituent classifiers are combined using the majority voting rule. The ensemble method is able to improve the accuracy of the individual classifiers. These basic classifiers include three hybrid approaches of artificial neural networks and metaheuristic algorithms, support vector machines and the k-nearest neighbors method. Although the model based on color information is computationally less expensive, it is only able to achieve a correct classification rate of 95.12%. In contrast, the optimal selection of the spectral bands corresponds to the range from 465 to 485 nm, which achieves a very precise result of 99.37% CCR, and proving also to be very stable in different executions. It is shown that selecting a narrow band is more adequate than using the full spectral data, since the ANN model using the range from 450 to 1000 nm is only able to achieve a 92.12% CCR. It also has to be considered that this method uses a different approach, not based on ensemble classifiers, which could partly explain its poor results.

As a future work, it would be interesting to verify these results with much larger datasets. In our case, the small number of available samples was compensated with the repetition of the training/test process 1000 times for each method. Data augmentation techniques could be applied to obtain more artificial samples, which would be required by deep learning methods; this was not considered necessary in the traditional neural networks used in the present study. In any case, with the inclusion of more varied samples and varieties, and also in different domains, new sources of variability in the spectra could appear that cannot be generated just with data augmentation methods.

Another important line of research is related to the application of the proposed method in natural outdoor conditions. In the present work, the apples were analyzed under controlled laboratory settings. New challenges and difficulties would appear in a practical in-field application, for example using drones or satellite imagery.

Funding

This research was funded by the European Union (EU) under Erasmus+ project entitled "Fostering Internationalization in Agricultural Engineering in Iran and Russia" [FARmER] with grant number 585596-EPP-1-2017-1-DE-EPPKA2-CBHE-JP. It was also funded by the Spanish MICINN, as well as European Commission FEDER funds, under grant RTI2018-098156-B-C53.

References

Adebayo, S. E., Hashim, N., Abdan, K., & Hanafi, M. (2016). Application and potential ofbackscattering imaging techniques in agricultural and food processing—a review. *journal of Food Engineering, 169*, 155–164.

Adi, D. D., Oduro, I. n., & Tortoe, C. (2019). Physicochemical changes in plantain during normal storage ripening. *Scientific African, 6*, 00164.

Arendse, E., Fawole, O. A., Magwaza, L. S., & Opara, U. L. (2018). Non-destructive prediction of internal and external quality attributes of fruit with thick rind: A review. *J. Food Engineering, 217*, 11–23.

Bhuvaneswari, P., & Therese, A. B. (2015). Detection of Cancer in Lung With K-NN Classification Using Genetic Algorithm. *Procedia Materials Science, 10*, 433-440.

Bizzani, M., Flores, D. W. M., Colnago, L. A., & Ferreira, M. D. (2017). Non-invasive spectroscopic methods to estimate orange firmness, peel thickness, and total pectin content. . *Microc*. doi: 10.1016/j.microc.2017.03.039

Cardenas-Perez, S., Chanona-Perez, J., Mendez-Mendez, J. V., Calderon-Domínguez, G., Lopez-Santiago, R., Perea-Flores, M. J., & Arzate-Vazquez, I. (2017). Evaluation of the ripening stages of apple (Golden Delicious) by means of computer vision system. *Biosystem Engineering, 159*, 46-58.

Cavaco, A. M., Pires, R., Antunes, M. D., Panagopoulos, T., Brázio, A., Afonso, A. M., Guerra, R. (2018). Validation of short wave near infrared calibration models for the quality and ripening of 'Newhall' orange on tree across years and orchards. *Postharvest Biology and Technology, 141*, 86-97.

Cayuela, J. A. (2008). Vis–NIR soluble solids prediction in intact oranges (Citrus sinensis L.) cv. Valencia Late by reflectance. *Postharvest Biol Technol, 47*, 75–80.

Clerici, M. T. P. S., Kallmann, C., Gaspi, F. O. G., Morgano, M. A., Martinez-Bustos, F., & Chang, Y. K. (2011). Physical, chemical and technological characteristics of Solanum lycocarpum A. St. - HILL (Solanaceae) fruit flour and starch. *Food Research International 44* 2143–2150.

Cortes, C., & Vapnik, V. (1995). *Machine Learning* (Vol. 20).

Fernandez-Novales, J., Garde-Cerdan, T., Tardaguila, J., Gutierrez-Gambo, G., Perez-Alvarez, E., & Diago, M. P. (2019). Assessment of amino acids and total soluble solids in intact grape berries using contactless Vis and NIR spectroscopy during ripening. *Talanta, 199*, 244-253.

García-Mateos, G., Hernández-Hernández, J. L., Escarabajal-Henarejos, D., Jaén-Terrones, S., & Molina-Martínez, J. M. (2015). Study and comparison of color models for automatic image analysis in irrigation management applications. Agricultural Water Management, 151, 158-166.

Garg, H. (2016). A hybrid PSO-GA algorithm for constrained optimization problems. *Applied Mathematics and Computation, 274*, 295-305.

Hernández-Hernández, J. L., Ruiz-Hernández, J., García-Mateos, G., González-Esquiva, J. M., Ruiz-Canales, A., & Molina-Martínez, J. M. (2017). A new portable application for automatic segmentation of plants in agriculture. Agricultural Water Management, 183, 146-157.

Kennedy, J., & Eberhart, R. (1995). *Particle Swarm Optimization*. Paper presented at the Proceedings of the IEEE International Conference on Neural Networks, Perth, Australia.

Lamikanra, O. (2002). *Fresh-cut fruits and vegetables : science, technology, and market*. Boca Raton Fla: CRC.

Liu, C., Yang, S. X., & Deng, L. (2015). A comparative study for least angle regression on NIR spectra analysis to determine internal qualities of navel oranges. *Expert Syst. Appl., 42*, 8497–8503.

Martínez-Valdivieso, D., Font, R., Blanco-Díaz, M. T., Moreno-Rojas, J. M., Gómez, P., Alonso-Moraga, Á., & Río-Celestino, M. D. (2014). Application of near-infrared reflectance spectroscopy for predicting carotenoid content in summer squash fruit. *Computers and Electronics in Agriculture, 108* 71–79.

Mohammadi, V., Kheiralipour, K., & Ghasemi-Varnamkhasti, M. (2015). Detecting maturity of persimmon fruit based on image processing technique. *Scientia Horticulturae, 184* 123–128.

Ncama, K., Opara, U. L., Tesfay, S. Z., Fawole, O. A., & Magwaza, L. S. (2017). Application of Vis/NIR spectroscopy for predicting sweetness and flavour parameters of 'Valencia'

orange (Citrus sinensis) and ‘Star Ruby’ grapefruit (Citrus x paradisi Macfad). *Journal of Food Engineering, 193* 86-94.
Nicolaï, B. M., Beullens, K., Bobelyn, E., Peirs, A., Saeys, W., & Theron, I. K. (2007). Non-destructive measurement of fruit and vegetable quality by means of NIR spectroscopy: A review. *Postharvest Biology and Technology, 46*, 99–118.
Pourdarbani, R., Sabzi, S., Hernández-Hernández, J., Hernández-Hernández, M., & García-Mateos, G. (2019). Comparison of Different Classifiers and the Majority Voting Rule for the Detection of Plum Fruits in Garden Conditions. *Remote sensing, 11*, 2546. doi: 10.3390/rs11212546
Pourdarbani, R., Sabzi, S., Kalantari, D., Hernández-Hernández, J., & Arribas, J. (2020). A Computer Vision System Based on Majority-Voting Ensemble Neural Network for the Automatic Classification of Three Chickpea Varieties. *Foods 9*(2), 113.
Rossel, R. A. V. (2008). ParLeS: Software for chemometric analysis of spectroscopic data. *Chemometrics and Intelligent Laboratory Systems, 90*, 72–83.
Sabzi, S., Abbaspour-Gilandeh, Y., García-Mateos, G., Ruiz-Canales, A., & Molina-Martínez, J. M. (2018). Segmentation of apples in aerial images under sixteen different lighting conditions using color and texture for optimal irrigation. *Water, 10*, 1634. doi: 10.3390/w10111634
Sabzi, S., Abbaspour-Gilandeh, Y., García-Mateos, G., Ruiz-Canales, A., Molina-Martínez, J. M., & Arribas, J. I. (2019). An Automatic Non-Destructive Method for the Classification of the Ripeness Stage of Red Delicious Apples in Orchards Using Aerial Video. *Agronomy, 9*, 84. doi: 10.3390/agronomy9020084
Sabzi, S., Abbaspour-Gilandeh, Y. (2018). Using video processing to classify potato plant and three types of weed using hybrid of artificial neural network and partincle swarm algorithm. *Measurement, 126*, 22–36.
Sabzi, S., Javadikia, P., Rabbani, H., Adelkhani, A., Naderloo, L. (2013). *Agricultural Engineering International: CIGR Journal 15* (4), 213–219.
Tian, Y., Yang, G., Wang, Z., Wang, H., Li, E., & Liang, Z. (2019). Apple detection during different growth stages in orchards using the improved YOLO-V3 model. *Computers and Electronics in Agriculture, 157*, 417–426.
Torres, I., Perez-Marin, D., Haba, M. J. D. l., & Sanchez, M. T. (2017). Developing universal models for the prediction of physical quality in citrus fruits analysed on-tree using portable NIRS sensors. *Biosystems engineering, 153*, 140–148.
Yang, X.-S. (2009). *Firefly algorithms for multimodal optimization*. Paper presented at the Stochastic Algorithms: Foundations and Applications, SAGA 2009, Lecture Notes in Computer Sciences.

This document corresponds to the accepted manuscript of the article published in Computers and Electronics in Agriculture (Elsevier) in 2020.
The final published version is available at: https://doi.org/10.1016/j.compag.2020.105643